

Supporting Online Material

Triboluminescence Flashes from High-Speed Ruptures in Carbon Nanotube Macro-Yarns

Thurid S. Gspann^{a*}, Nigel H.H. Ngern^b, Andrew Fowler^a, Alan H. Windle^a, Vincent B.C. Tan^b, James A. Elliott^a

^a Department of Materials Science and Metallurgy, University of Cambridge, 27 Charles Babbage Road, CB3 0FS Cambridge, UK

^b Department of Mechanical Engineering, National University of Singapore, 9 Engineering Drive 1, Singapore 117576

Sample Cross-sections

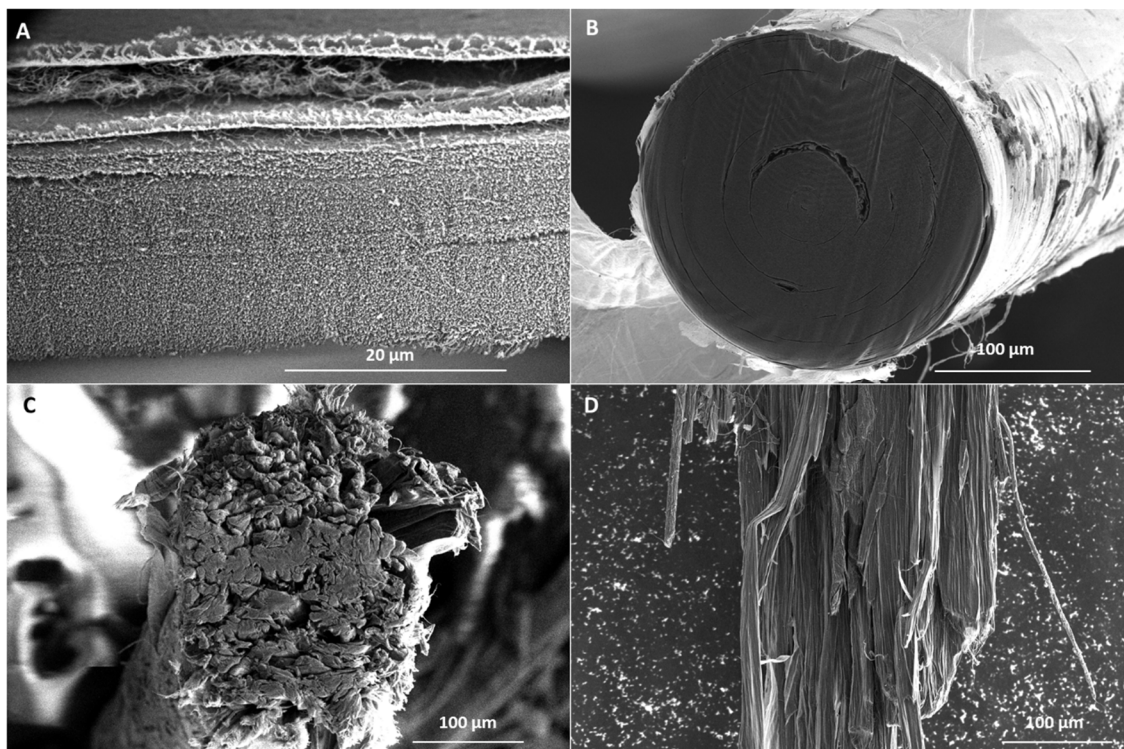


Figure S1: (A) Cross-section of a CNT ribbon. The thickness is made up of thin network layers continuously spun and layered up. The top layers in this image lift off as the sample was pressed between glass slides for laser cutting of the cross section. (B) Cross section of a CNT Rolled Rope showing a very dense cross section, sporadically with larger inter-layer distances caused by either impurities or handling. (C) Cross section of a CNT Tow composed of individually condensed fibres rolled together. (D) Top view of a CNT Tow after being submitted to a tensile test, depicting one-by-one filament breakage.

The electron micrographs in figures 4 and S1 – S3 were recorded with a FEI Nova NanoSEM using 5 keV, with the exception of figure S1A, which was focused ion beam cut (30 keV) and imaged in a FEI Helios NanoLab microscope.

* **Corresponding Author:** Thurid Gspann, tsg28@cam.ac.uk

Quasi-static fracture – Fibrous Pull-out

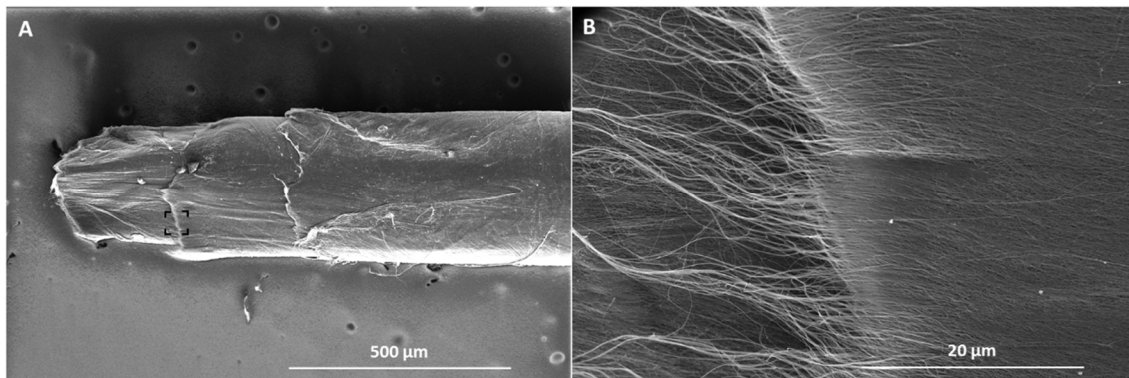


Figure S2: CNT rope fractured in a quasi-static tensile test at a strain rate of 0.0016 /sec. (A) shows the sheath-and-core failure typical for rolled ropes. The magnified section in (B) shows the fibrous pull-out typical for CNT network failure.

Dynamic fracture – Scorched surfaces

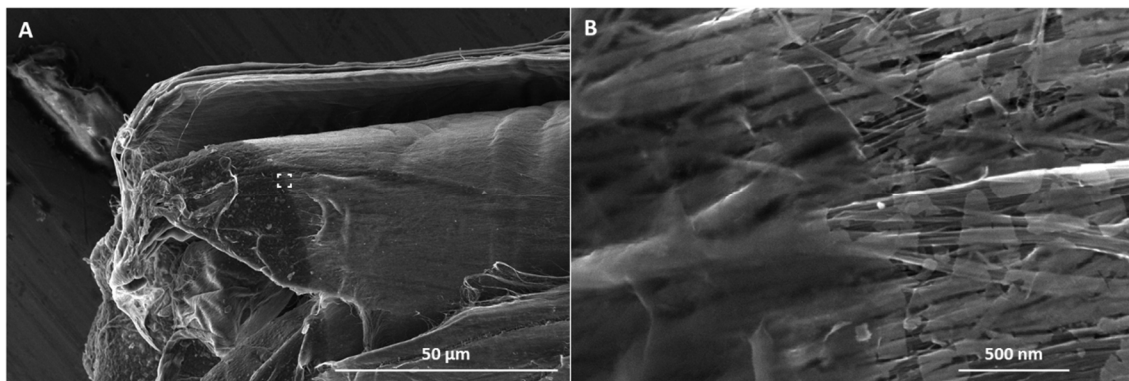


Figure S3: CNT rope fractured in a dynamic tensile test at a strain rate of 500 sec⁻¹. (A) shows the fracture surface, partly scorched and covered with a molten looking substance, (B) shows the boundary between said scorched region and a region covered in lighter patches. We interpret this phenomenon as zones of different temperature, where in (A) the temperature is so high that CNTs are possibly destroyed and the polymeric bundle coating melts, while in (B) the bundle coating is transformed possibly cross-linked on air into a brittle coating.

Calculation of Thermal Decay Time

We can calculate the thermal decay time, t_D , according to:

$$t_D = A_{flash}/\alpha$$

with A_{flash} being the area of the flash and α being the thermal diffusivity. As the flashes are only recorded over a single pixel and a single frame, we assume an area of $(27 \mu\text{m})^2$ which corresponds to the pixel resolution of the high-speed camera used and is a good approximation for the sub-elements of the tows, shown in Figure S1-D.

Up to 400 K, the thermal diffusivity of CNT macrostructures has been shown to follow the relationship $\alpha = \kappa^* \cdot C_V$, with the specific heat capacity, $C_V = 2.56 \cdot T - 61.73$, being approximately linear independent of CNT type or their agglomeration into films or ropes [1] [2]. Using the thermal conductivity reported in [3], we calculate a thermal decay time of between 0.42 – 1.10 μs, which is shorter than one high-speed camera frame duration.

Above the Debye temperature, which for carbon nanotubes is close to room temperature [3], the thermal conductivity will decrease due to phonon scattering steeper than T^{-1} [4], but this effect will be counteracted by the increase of specific heat capacity, saturating for high temperatures (above $T_{Umklapp}$) according to the Debye model. Although no experimental data are available, we can conservatively estimate the decay time to be $< 2 \mu\text{s}$ for temperatures up to 2000 K, which is far above the thermal decomposition temperature of CNTs in air known from TGA (400 - 700 K).

For the calculations below, we set the thermal decay time limits as 0.4 – 2.5 μs , using a conservative estimate for the upper limit. The latter is larger than the duration of one high-speed camera frame; however, if the flash occurrence is caused by gas bubble combustion rather than by black body radiation of a glowing CNT network, the duration of the flash is likely to be much shorter than the thermal decay time in the CNT network.

Calculation of Initial Black Body Temperature of Flash Event

A_{flash}	Area over which flash is observed (i.e. pixel area of the high-speed camera)
A_{IR}	Pixel area of the IR camera
t_D	Flash decay time t_D (Frame duration of the high-speed camera t_{HSC})
t_{exp}	Exposure time of IR camera frame
$prediction(\lambda)$	Energy anticipated by linear combination of flash and background
$measured(\lambda)$	Energy measured by the IR camera
T_0	Initial temperature at flash
T_{BG}	Background temperature
T_{IR}	Temperature of the IR pixel measured
$E(\lambda)$	Total energy emitted
$B(\lambda, T(t))$	Radiance per unit wavelength
λ	Wavelength

The temperatures were read from the IR camera assuming an emissivity of 0.7. As shown by [5], near-perfect black body radiation only applies for the top surface of CNT forests, the more perpendicular the incident angle to the CNT axis, the higher is the reflectance, thereby reducing the emissivity value to as low as 0.7 for pressed films or buckypapers.

We assume that one flash event coincides with the IR camera pixel showing the highest temperature at fracture. The ratio of the one high-speed camera pixel A_{flash} to IR camera area A_{IR} is:

$$\frac{A_{flash}}{A_{IR}} = \frac{(27 \mu\text{m})^2}{(180 \mu\text{m})^2} = \frac{1}{44.4} \quad (1)$$

The ratio of the duration of the high-speed camera's frame t_{HSC} to integration time per pixel set for the IR camera t_{exp} is:

$$\frac{t_{HSC}}{t_{exp}} = \frac{1.25}{10} \quad (2)$$

As we observe the flashes over one high-speed camera frame, we set the decay time to $t_D = t_{HSC}$.

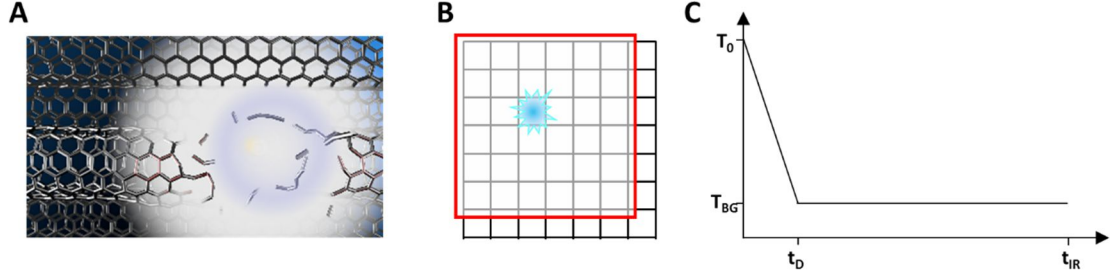


Figure S4: Schematic depicting the calculations for an initial temperature of a filament in a tow breaking (A). (B) The event recorded in one high-speed camera pixel (black) spans only a fraction of the IR camera pixel (red). (C) The initial temperature decays over a characteristic thermal decay time t_D to the background temperature.

We consider the energy measured by one flashing pixel over an exposure time t_{exp} as a linear combination of the background and a flash black body emission $B(\lambda, T(t))$.

$$prediction(\lambda) = \underbrace{A_{flash} \left(\int_0^{t_D} B(\lambda, T(t)) dt + \int_{t_D}^{t_{exp}} B(\lambda, T_{BG}(t)) dt \right)}_{\text{Flash}} + \underbrace{(A_{IR} - A_{flash}) \int_0^{t_{exp}} B(\lambda, T_{BG}(t)) dt}_{\text{Background}} \quad (3)$$

We assume that the temperature in the flash region A_{flash} decays from some initial unknown temperature T_0 to the background temperature T_{BG} over time t_D . Simplifying, we see that

$$prediction(\lambda) = A_{flash} \int_0^{t_D} B(\lambda, T(t)) dt + ([t_{exp} A_{IR} - t_D A_{flash}] B(\lambda, T_{BG})) \quad (4)$$

We need to find the cumulative energy emitted by a decaying black body per unit area and for wavelength λ

$$E(\lambda) = \int_0^{t_D} B(\lambda, T(t)) dt \quad (5)$$

where for Planck's law we show an implicit dependence of the black body temperature $T(t)$ upon time t .

$$B(\lambda, T) = \frac{2 \cdot hc}{\lambda^5} \frac{1}{e^{\frac{hc}{\lambda k T}} - 1} \quad (6)$$

with k the Boltzmann constant, h the Planck constant, c the speed of light in the medium, here air. We assume a linear decay of the black body temperature:

$$T(t) = T_0 + (T_{BG} - T_0) \frac{t}{t_D} \quad (7)$$

and utilise

$$\frac{dT}{dt} = \frac{T_{BG} - T_0}{t_D} \quad (8)$$

To rephrase (5) as

$$E(\lambda) = \frac{t_D}{T_{BG} - T_0} \int_{T_0}^{T_{BG}} B(\lambda, T) dT \quad (9)$$

We calculate (9) numerically with SciPy's quadrature routine [6] and introduce:

$$\tilde{E}(\lambda, T_{BG}, T_0) = \frac{1}{T_{BG} - T_0} \int_{T_0}^{T_{BG}} B(\lambda, T) dT \quad (10)$$

Then,

$$prediction(\lambda) = (A_{flash} t_D) \tilde{E}(\lambda, T_{BG}, T_0) + ([t_{exp} A_{IR} - t_D A_{flash}] B(\lambda, T_{BG})) \quad (11)$$

We compare our anticipated distribution $prediction(\lambda)$ with the measured distribution $measured(\lambda)$ from the IR camera assuming a single black body

$$measured(\lambda) = t_{exp} A_{IR} B(\lambda, T_{IR}) \quad (12)$$

Since the IR camera measures only the total energy emitted in the region $\lambda = [\lambda_{min}, \lambda_{max}] = [2.5\mu\text{m}, 5.1\mu\text{m}]$ we compare total energies over our bandwidth for $B(\lambda, T_{IR})$ and

$$\begin{aligned} \tilde{B}(\lambda, T_{BG}, T_0) &= \frac{prediction(\lambda)}{t_{exp} A_{IR}} \\ &= \left(\frac{A_{flash}}{A_{IR}} \right) \left(\frac{t_D}{t_{exp}} \right) \tilde{E}(\lambda, T_{BG}, T_0) + \left(1 - \left(\frac{A_{flash}}{A_{IR}} \right) \left(\frac{t_D}{t_{exp}} \right) \right) B(\lambda, T_{BG}) \end{aligned} \quad (13)$$

Finally, we perform a minimisation of:

$$\left| \int_{\lambda_{min}}^{\lambda_{max}} B(\lambda, T_{IR}) d\lambda - \int_{\lambda_{min}}^{\lambda_{max}} \tilde{B}(\lambda, T_{BG}, T_0) d\lambda \right| \quad (14)$$

by varying T_0 where the integrals over λ are performed numerically with Simpson's rule.

From examination of the IR camera measurements, we divide the measurements into two populations: Five measurements were collected just before the actual break, mainly tows. Their temperature is calculated to be (1100 ± 270) K (figure S6). However, the area in this case is overestimated as the individual elements comprising a tow are filaments of $10 \mu\text{m}$ diameter, which is smaller than a high-speed camera pixel. Hence the actual temperature is likely to be higher.

The IR frames of the second population (11 measurements) were recorded just after the break comprises mainly ropes and ribbons, with temperatures of (1620 ± 750) K and (2910 ± 1230) K, respectively. In case of ribbons, the number of flash events is likely to be larger than one, as we could capture the fracture as the crack progresses through the ribbon's width, increasing the probability to record one or several flashes during one IR camera frame (figure S6). The temperature of the individual event is therefore likely to be overestimated by this method.

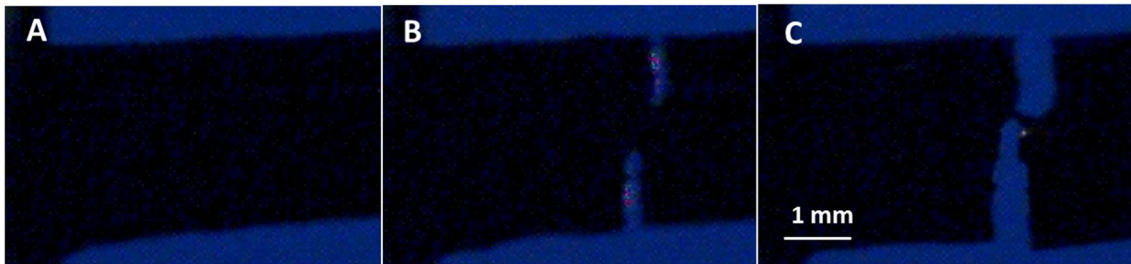


Figure S5: (A) A CNT ribbon under tension with a strain rate of 1/sec just before fracture, (B) fracture of the ribbon showing several flashes along the fracture edges, and (C) final rupture of the ribbon, showing one more single flash event.

In summary, we find that the initial flash black body temperature T_0 calculated by the method in (14) is highly sensitive to the area and time ratios A_{flash}/A_{IR} and t_D/t_{exp} . Since these are not known to the degree of accuracy necessary in (12), we instead consider a range of physically possible ratios $A_{flash} = [A_{min}; A_{max}]$, $t_D = [t_{min}; t_{max}]$ for each experiment.

For A_{flash} , we use $A_{min} = (10 \mu\text{m})^2$ for the diameter of the individually condensed fibres comprising the tows as the smallest element fracturing, and $A_{max} = (27 \mu\text{m})^2$ as we observe the flashes over one high-speed camera pixel. For ribbons, we allow A_{max} to span arbitrarily over 5 pixels. The lower and upper limits of t_D were set to $0.4 \mu\text{s}$ and $2.5 \mu\text{s}$, as discussed above.

Our method now proceeds by assuming all observed flashes have the same initial black body temperature, T_0 . For a given flash (T_{BG} ; T_{IR} ; A_{max} ; t_{max}) and initial flash temperature T_0 , minimise (14) by varying A_{flash}/A_{IR} and t_D/t_{exp} within $A_{flash} = [A_{min}; A_{max}]$ and $t_D = [t_{min}; t_{max}]$, respectively. If the expression in (14) equals zero in this range, then a flash of initial temperature T_0 is possible. We repeat this for all samples measured and for an arbitrary selection of flash temperatures T_0 .

Although we cannot give a precise initial flash temperature, we can however say if a given initial flash temperature is possible within our model.

Now, for tows and ribbons, the possible initial temperature solutions T_0 peak around 1800 K. A wide range of higher temperatures is possible as solution for ribbon samples for which the number of flash events per IR camera pixel is likely higher, however, unknown.

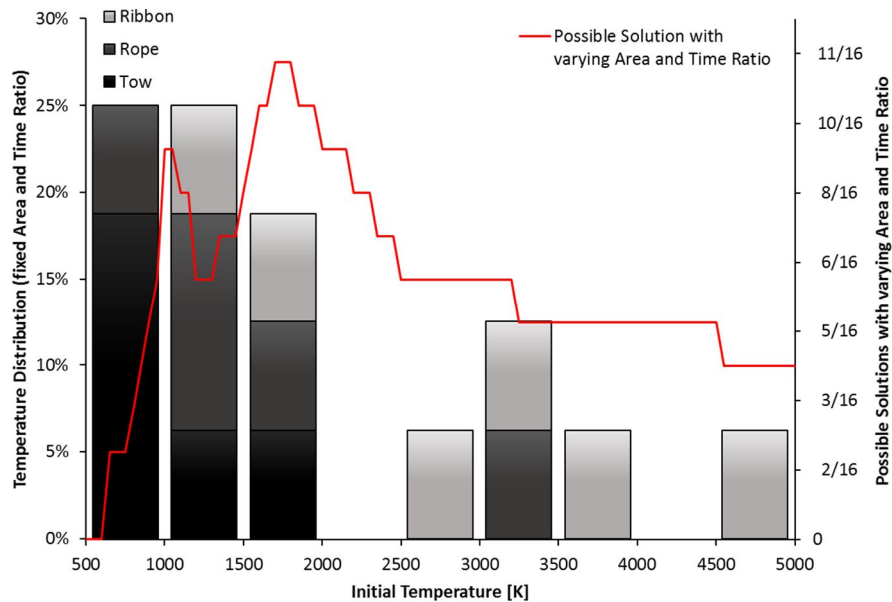


Figure S6: Block distribution of temperatures with $A_{flash}/A_{IR} = 1/44.4$ and $t_D/t_{exp} = 1.25/10$. Red: Possible temperature solutions T_0 with variable area and time ratios within the specified limits.

Shielding the sample from contact with air

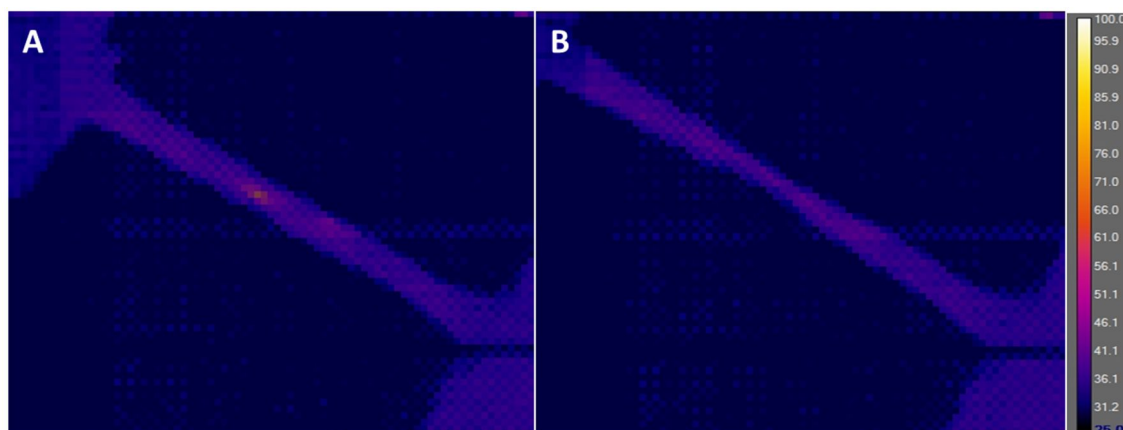


Figure S7: FLIR images of a uncured polymer coated CNT ribbon (A) close to fracture, and (B) after fracture. In contrast to the uncoated samples shown in Figure 2, no significant heating was observed. The colour chart is given in °C.

Videos:

- Rope: Very bright flash
- Tow: up to >20 individual flashes
- Ribbon: Large flash
- IR camera video of a CNT ribbon
- IR camera video of a CNT rope

References

- [1] N. R. Pradhan, H. Duan, J. Liang and G. S. Iannacchione, *Nanotechnology* **20**, 245705 (2009).
- [2] S. Hepplestone, A. Ciavarella, C. Janke and G. Srivastava, *Surface Science* **600**, 18, 3633 (2006).
- [3] T. S. Gspann, S. M. Juckes, J. F. Niven, M. B. Johnson, J. A. Elliott, M. A. White and A. H. Windle, *Carbon* **114**, 160 (2017).
- [4] E. Pop, D. Mann, Q. Wang, K. Goodson and H. Dai, *Nano Letters* **6**, 1, 96 (2006).
- [5] K. Mizuno, J. Ishii, H. Kishida, Y. Hayamizu, S. Yasuda, D. N. Futaba, M. Yumura and K. Hata, *PNAS* **106**, 15, 6044 (2009).
- [6] E. Jones, E. Oliphant and P. Peterson, *SciPy: Open Source Scientific Tools for Python* (2001).